Reprinted from Journal of Biomechanics, Vol 35, Saikko, V. and Calonius, O., Slide track analysis of the relative motion between femoral head and acetabular cup in walking and in hip simulators, Pages 455-464, Copyright (2002), with permission from Elsevier Science.

ELSEVIER

Journal of Biomechanics 35 (2002) 455–464

JOURNAL OF BIOMECHANICS

www.elsevier.com/locate/jbiomech
www.JBiomech.com

Slide track analysis of the relative motion between femoral head and acetabular cup in walking and in hip simulators

Vesa Saikko*, Olof Calonius

Laboratory of Machine Design, Department of Mechanical Engineering, Helsinki University of Technology, P.O. Box 4300, 02015 HUT, Finland

Accepted 28 November 2001

Abstract

Joint simulators are important tools in wear studies of prosthetic joint materials. The type of motion in a joint simulator is crucial with respect to the wear produced. It is widely accepted that only multidirectional motion yields realistic wear for polyethylene acetabular cups. Multidirectionality, however, is a wide concept. The type of multidirectional motion varies considerably between simulators, which may explain the large differences in observed wear rates. At present, little is known about the relationship between the type of multidirectional motion and wear. One illustrative way to compare the motions of various hip simulators is to compute tracks made on the counterface by selected points of the surface of the femoral head and acetabular cup due to the cyclic relative motion. A new computation method, based on Euler angles, was developed, and used to compute slide tracks for the three-axis motion of the hip joint in walking, and for two hip simulators, the HUT-3 and the biaxial rocking motion. The slide track patterns resulting from the gait waveforms were found to be similar to those produced by the HUT-3 simulator. This paper is the first to include a verification of the computed simulator tracks. The tracks were verified in the two simulators using sharp pins, embedded in acetabular cups, engraving distinct grooves onto the femoral heads. The engravings were identical to the computed tracks. The results clearly differed from earlier computations by another research group. This study is intended to start a thorough investigation of the relationship between the type of multidirectional motion and wear.

Keywords: Slide track; Hip simulator; Euler angle; Multidirectional motion; Wear

1. Introduction

The wear of total hip prostheses can be studied using hip joint simulators and hip wear simulators. In hip joint simulators, actual total hip prostheses are tested in conditions resembling as closely as possible those prevailing in the human body, usually in walking (Dowson and Jobbins, 1988; Saikko, 1996; Ungethüm et al., 1973). In hip wear simulators, either total hip prostheses are tested in conditions which less rigorously follow the true conditions, to make the device less complex (McKellop et al., 1995; Saikko et al., 2001; Wang et al., 1997), or specimens of simplified geometry, such as pin on disk, are used, but the test conditions are tailored to yield realistic hip wear mechanisms (Saikko, 1998). Existing simulators greatly differ from each other with respect to test conditions, that is, motion, load, and lubrication. The wear of the most common acetabular cup material, ultra-high molecular weight polyethylene, has been found to be highly sensitive to the type of motion and lubricant. Multidirectional motion and protein-containing lubricant result in realistic wear mechanisms (McKellop et al., 1995; Saikko, 1998; Wang et al., 1997). The type of load is less important (Saikko and Ahlroos, 1999). The type of multidirectional motion varies between simulators, which may partly explain the large differences in the observed wear rates. Moreover, it has been suggested that the variation in gait between patients may partly explain the substantial variation in clinical wear rates of total hip prostheses (Bennett et al., 2000). Research on the relationship between the type of multidirectional motion and wear is scarce.

In 1993, Saikko designed a three-axis hip joint simulator called HUT-3, which was described in Saikko (1996). The electrogoniometric measurements of the hip joint in walking by Johnston and Smidt (1969) formed the basis in the design of the motion waveforms (Fig. 1). The amplitudes of FE, AA and IER are 46°, 12° and

*Corresponding author. Tel.: +358-9-451-3562; fax: +358-9-451-3542.

E-mail address: vesa.saikko@hut.fi (V. Saikko).

0021-9290/02/$ - see front matter
PII: S0021-9290(01)00224-X

Nomenclature

L	joint contact resultant force
r	radius of femoral head
t	time
T	cycle time
τ_μ	tangential shear stress at articulating surface caused by friction
FE	flexion-extension
AA	abduction–adduction
IER	internal–external rotation
BRM	biaxial rocking motion
HUT-3	Helsinki University of Technology hip joint simulator Mark III
Slide track	track made on the counterface by a point on the surface of femoral head or acetabular cup due to cyclic relative motion
Force track	track made on the femoral head by the point of theoretical joint contact resultant force, which is fixed relative to the cup in the cases studied
Aspect ratio	major dimension divided by minor dimension of a slide track figure

12°, respectively, the phase difference between FE and AA being $\pi/2$. Heel strike occurs 0.1 T after maximum flexion, and toe-off 0.1 T after maximum extension. The most popular hip wear simulator is the so-called biaxial rocking motion (BRM) principle (McKellop et al., 1995; Saikko and Ahlroos, 1999; Wang et al., 1997). This design can be defined as having two motion components, FE and AA. Their phase difference is $\pi/2$, but they are both sinusoidal with an amplitude of 46° (Fig. 1). The excessive AA is a 'penalty' for the simple, clever mechanism, which makes it possible to build a compact multistation device. In the different commercial BRM simulators, the load axis is always vertical and the lower component is the moving one, but the joint may be either upright or upside down. The rotation of the leaning shaft has been prevented using various kinds of levers. The shape of the rotation-prevention lever is likely to affect the relative motion. Many different load waveforms have been used, even static load by the present authors (Saikko and Ahlroos, 1999; Saikko et al., 2001). Since the 1980s, hundreds of BRM test stations have been employed around the world.

The motion produced by a simulator can be illustrated by computing tracks made on the counterface by selected points of the surface of femoral head and acetabular cup due to the cyclic relative motion. Earlier computations of this kind (Ramamurti et al., 1996, 1998) are inconclusive because the papers contain no mention of any verification. The computations of three-axis rotations are complex enough to contain a considerable risk of error. In the present study, a new method of computation was developed and used to compare slide tracks produced by the two simulators, HUT-3 and BRM, with each other and with those resulting from three-axis motion of the hip joint in walking (Johnston and Smidt, 1969). The computed hip simulator tracks were verified using sharp pins embedded into polyethylene cups. The pins engraved distinct grooves onto the femoral heads as one complete cycle was driven with the simulators. The grooves were compared with the computed tracks. The validity of the earlier computations is reviewed. In addition, the effect of slide tracks shapes on the wear rate produced by the two different simulators is discussed.

2. Methods

The numerical simulations were programmed and the results visualised using MATLAB (MathWorks, Inc., Natick, MA, USA). The relative motion between the femoral head and the acetabular cup was visualised with tracks drawn by a set of marker points on the surface of head and cup. The number of points was not restricted, and the location of the points could be freely selected. The principle followed in the selection of the number and location was to give an illustrative picture of the track pattern. Naturally, there are an infinite number of tracks, but too many tracks on one plot result in a tangled image. The variations of the FE, AA and IER angles are shown in Fig. 1. For the computation, each waveform was discretised using 100 points/cycle. The computation is described in detail in Appendix A.

The Euler sequence used in the computation from gait waveforms was FE→AA→IER, because the electrogoniometer used by Johnston and Smidt (1969) can be considered to conform with the definition of orthopaedic angles. The sequence used with the HUT-3 simulator was IER→AA→FE, according to the coordinate system of the design (Saikko, 1996). The initial position for gait and HUT-3 is shown in Fig. 2. With the BRM simulator (Fig. 3a), the sequence was FE→AA. The use of Euler angles means that each rotation changes the orientation of the two other axes (Lewis and Lew, 1977; Morrey and Chao, 1976; Ramakrishnan and Kadaba, 1991). Hence, the third rotation in the sequence occurs about an axis, the orientation of which has already changed twice.

The Euler sequence of rotations for any simulator design can be determined according to the following procedure, in which the rotations are made one at a time. The first rotation of the sequence is the one, which changes the orientation of the both remaining rotation

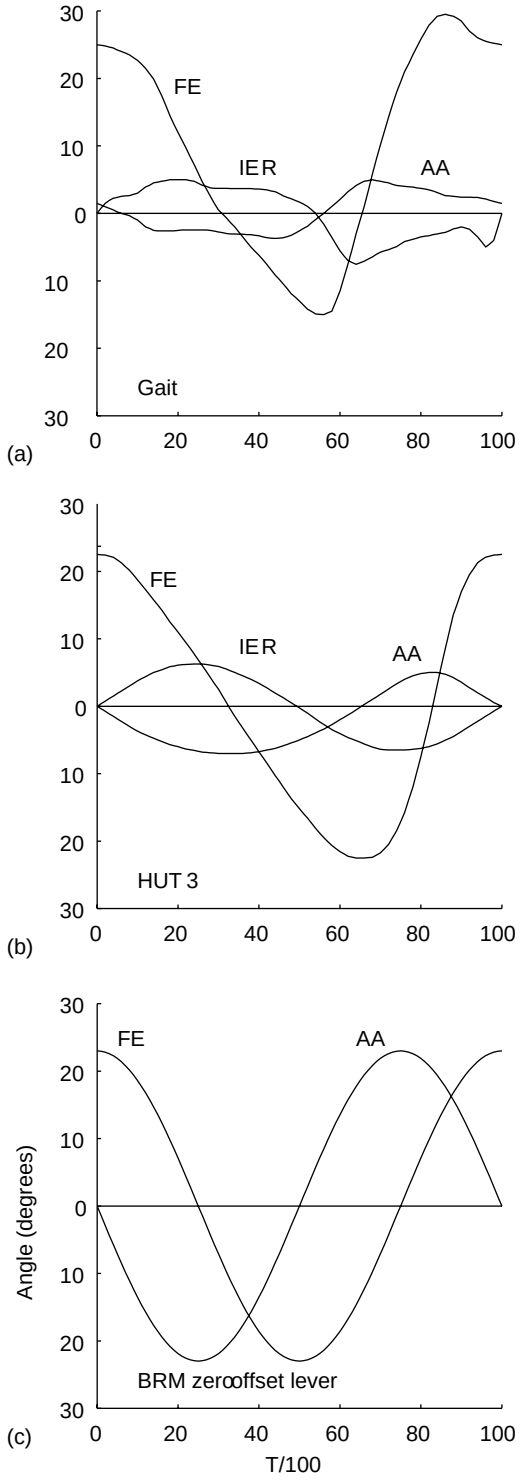

Fig. 1. Motion waveforms used in computation of slide tracks: (a) walking (from Johnston and Smidt, 1969), (b) HUT-3 simulator (from Saikko, 1996) and (c) BRM simulator. Positive angle represents flexion, abduction and internal rotation, and negative angle represents extension, adduction and external rotation.

axes of the simulator relative to the acetabular cup. This is because the reference coordinate system is fixed relative to the cup, as it is fixed relative to the pelvis in biomechanical studies of hip joint motion. Similarly, the

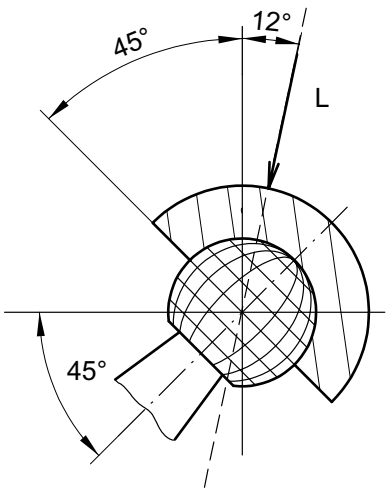

Fig. 2. Initial position of femoral head and acetabular cup, and direction of joint contact resultant force L (from Paul, 1976), in cases of walking and HUT-3 simulator. Right hip, coronal plane. It is irrelevant with respect to slide tracks produced that joint is actually upside down in HUT-3 simulator.

second rotation in the sequence is the one, which changes the orientation of the one remaining simulator axis relative to the cup. The third rotation in the sequence is the one which does not change the orientation of any simulator axis relative to the cup. In the case of a two-axis simulator, the first step in the procedure is skipped. The fact how the rotations are partitioned for the two components is unimportant because in tribology, it is the relative motion which counts. Determining the Euler sequence is an efficient way to enable an unequivocal analysis of any design and a direct comparison with any other design.

The computed tracks were verified by engraving 28 mm dia. CoCo femoral heads in the HUT-3 and BRM simulators. With the BRM simulator, two cases were studied: the rotation-prevention lever with and without offset (Figs. 3a and b), because in the commercial BRM simulators, the shape of the rotation-prevention lever varies. Sharp, hardened pins were embedded in several locations in polyethylene cups, 12 pins in HUT-3 and 17 pins in BRM (Fig. 4). The specimens and the whole test systems were then assembled and one cycle was driven with the load on. The grooves thus produced onto the heads were examined and measured using optical microscopy. For the photography, the grooves were accentuated with ink, and disturbing reflections of the polished ball surface were repressed.

3. Results

The slide track patterns resulting from gait waveforms (Fig. 5) were similar to those produced by the HUT-3

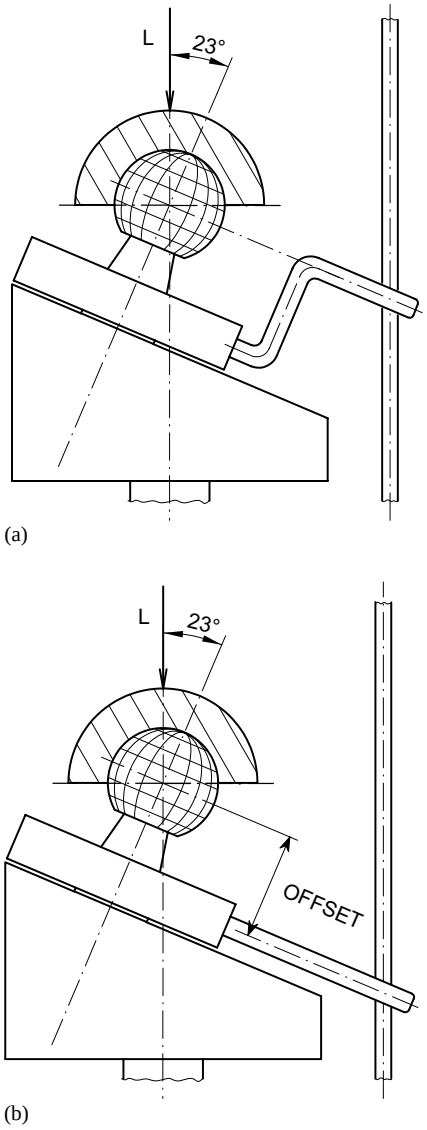

Fig. 3. Schematic of BRM simulator. Lever (a) without offset and (b) with offset.

simulator (Fig. 6). Most of the gait and HUT-3 slide tracks were oval, but there were also tracks with very high aspect ratio, and small track figures. The computed HUT-3 and BRM simulator slide tracks were in agreement with the engravings (Figs. 6–9). In the cases of three-axis motion (gait and HUT-3), the slide track pattern of the head was not identical to that of the cup (Figs. 5 and 6). In the case of two-axis motion (BRM), the slide track patterns of the head and the cup were identical, but their angular positions had a difference of $\pi/2$ (Fig. 8). The BRM slide track pattern was symmetric with respect to two perpendicular planes. The force track was circular. The tracks on the equator were figures of eight, bent figures of eight or straight lines. In between, the tracks included egg-shaped, nonsymmetric oval and elliptic figures. The aspect ratio

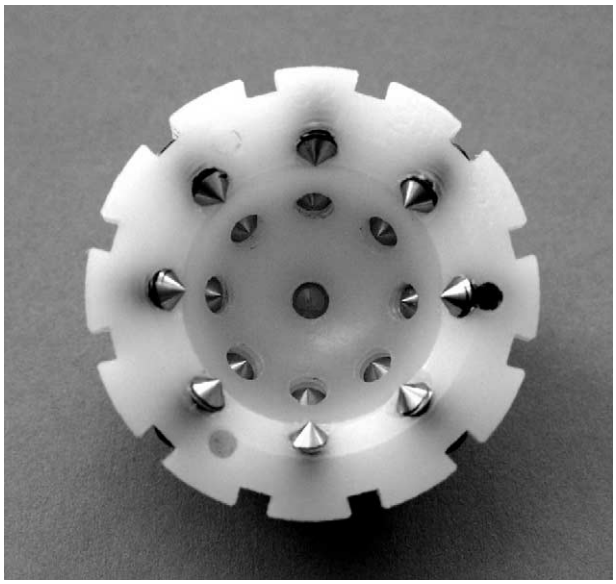

Fig. 4. Polyethylene acetabular cup, which was used to engrave femoral heads in BRM simulator with both types of rotation-prevention levers. There is one sharp, hardened pin on pole which engraves groove corresponding with force track, 8 pins equally distributed on 45° latitude, and 8 pins equally distributed on equator.

of the track figures increased towards the equator. Changing the type of rotation-prevention lever in the BRM simulator changed the pattern (Fig. 10). The lever with offset caused tilting and shift of grooves compared with the zero-offset case.

The lengths of the force tracks in walking, in the HUT-simulator and in the BRM simulator were $1.7r$, $1.7r$ and $2.5r$, respectively, and their aspect ratios 5.1, 3.8 and 1.0.

4. Discussion

This paper is the first to present computed slide tracks for hip simulators together with their verifications. Since the tracks computed for the two simulators were identical to the engraved grooves, it is most likely that the tracks computed from the gait waveforms were also correct, because the same method of computation was used in all three cases. Further, for the first time slide tracks were computed for both the head and the cup, and it was shown that in three-axis motion, the head and cup patterns differed, whereas in two-axis motion, they can be identical, the angular position being taken into account. Moreover, this paper is the first not only to present the true slide track pattern of the most popular hip wear simulator, BRM, but also to show that changing the shape of the rotation-prevention lever changes the pattern. This was additionally verified by holding a stationary drawing pen on various locations of the head while the head was doing the biaxial rocking motion without the cup.

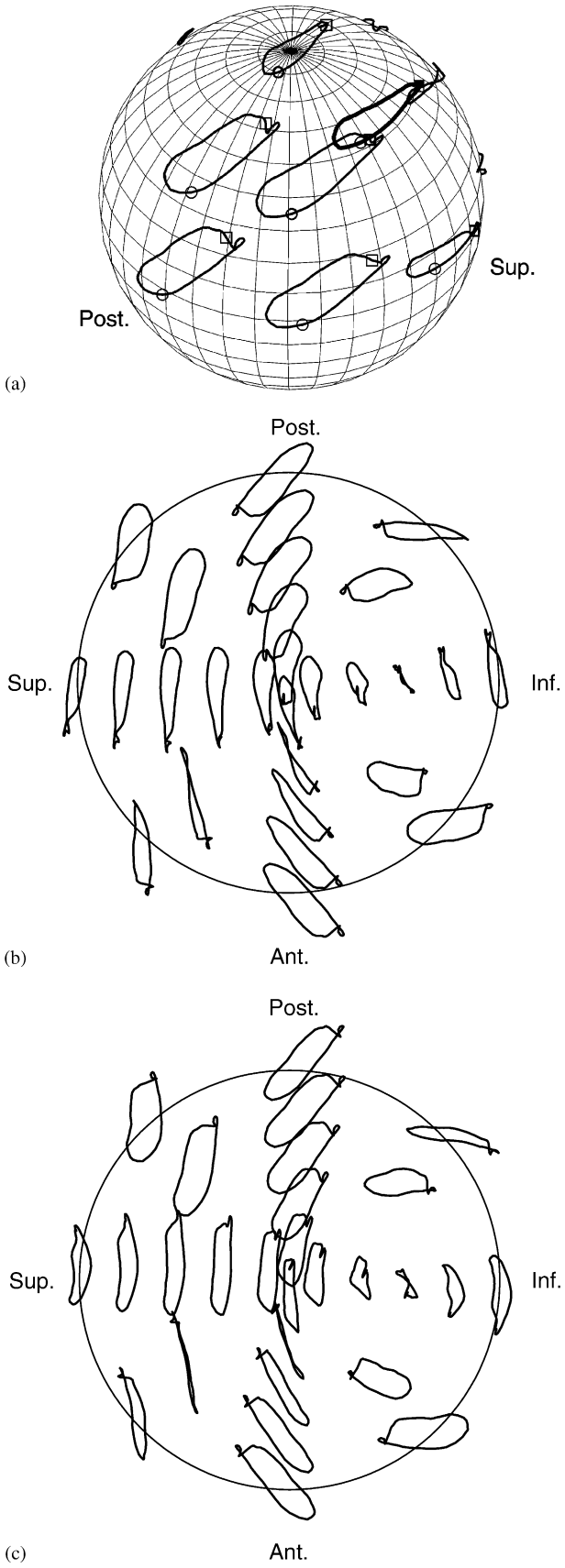

The similarity between the slide track pattern resulting from the hip joint motion in walking and that produced by the HUT-3 simulator is striking (Figs. 5 and 6). The result is logical considering the similarity in the motion waveforms regarding the amplitudes, and relative phases between the three motions (Fig. 1). The inverted Euler sequence of HUT-3 clearly has little influence, because the AA and IER amplitudes are small compared with the FE amplitude. As the HUT-3 waveforms were smoothened approximations of the gait waveforms, the HUT-3 slide tracks were naturally smoother, more elliptical than the gait tracks. For instance, the thorn in several gait tracks, which is due to a quick internal rotation just before heel strike, is not present in the HUT-3 tracks. The article describing the HUT-3 simulator (Saikko, 1996) was the first to include an engraved groove, corresponding with the force track. In addition to this, several other grooves were engraved in the present study. The aspect ratio of the elliptical force track, 3.8, was measured from the computed track and the engraved groove, but it was naturally equal to the ratio between the FE and AA amplitudes, 46/12, because the phase difference between FE and AA is $\pi/2$, and the influence of IER is small at the point of load application. It is sensible, however, to bear in mind the limitations of gait studies. The waveforms by Johnston and Smidt (1969) were obtained with a goniometer from normal subjects. The two principal problems of this goniometric study, which may have caused some error, were the slipping of the belt and elastic strap attachments, and the fact that the goniometer axes did not coincide with anatomical axes, especially with respect to AA and IER. In addition, the motion of a prosthetic hip joint may differ from that of a normal hip joint, not to mention the considerable patient-to-patient variation (Bennett et al., 2000).

The slide tracks produced by the BRM simulator clearly differed from the gait tracks (Figs. 5 and 8). Due to the longer tracks, the sliding velocity in the BRM simulator is higher than the average sliding velocity in walking and in the HUT-3 simulator, which increases frictional heating. This is caused by the excessive AA amplitude, 46°, of the BRM simulator. However, the BRM simulator has been shown to produce wear similar

Fig. 5. Slide tracks of selected points computed from gait waveforms, (a) on femoral head, force track drawn with thicker line, square indicating heel strike and circle indicating toe-off, and on flattened hemisphere surface of (b) femoral head and (c) acetabular cup. Hemispheres have been flattened so that shapes and sizes of slide tracks are not distorted. Radial distances correspond to distances measured from pole along spherical surface. Each track point was turned to plane about centre point of track in question. In (b) and (c), large circle represents equator, but due to flattening, its diameter is πr, not $2r$. In (c), tracks outside equator are only imaginary because there is no cup surface outside equator.

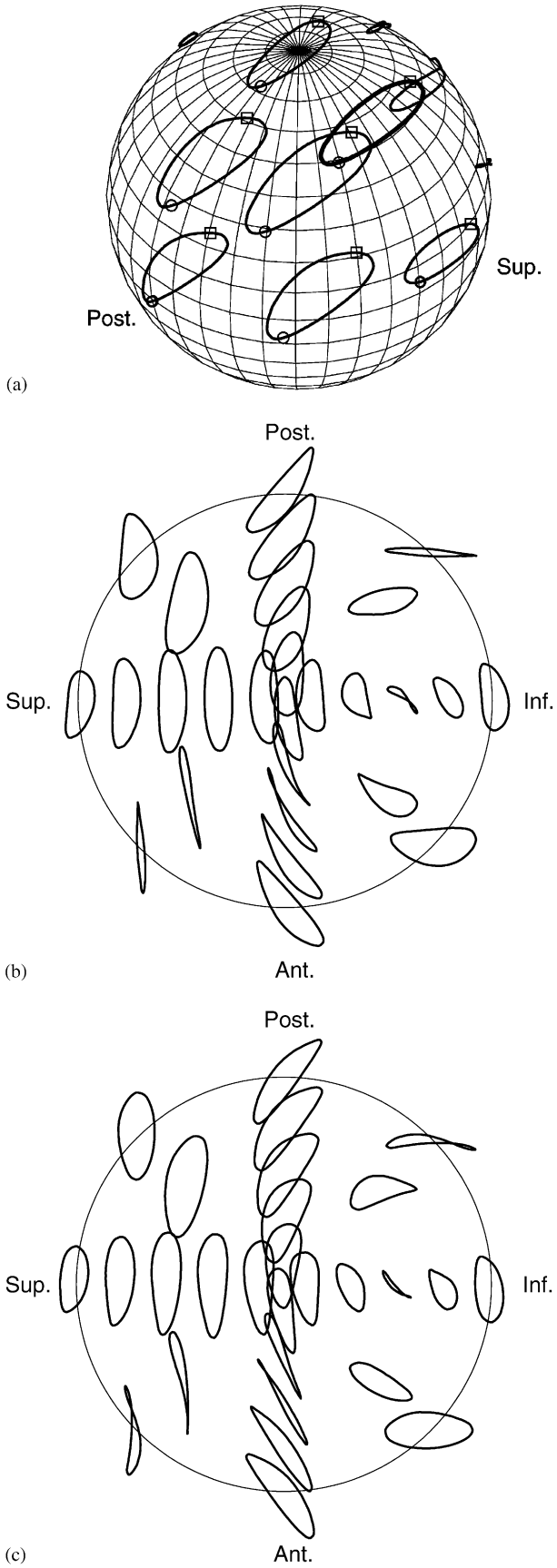

Fig. 6. Computed slide tracks of HUT-3 simulator, (a) on femoral head, and on flattened hemisphere surface of (b) femoral head and (c) acetabular cup. Points selected as in Fig 5.

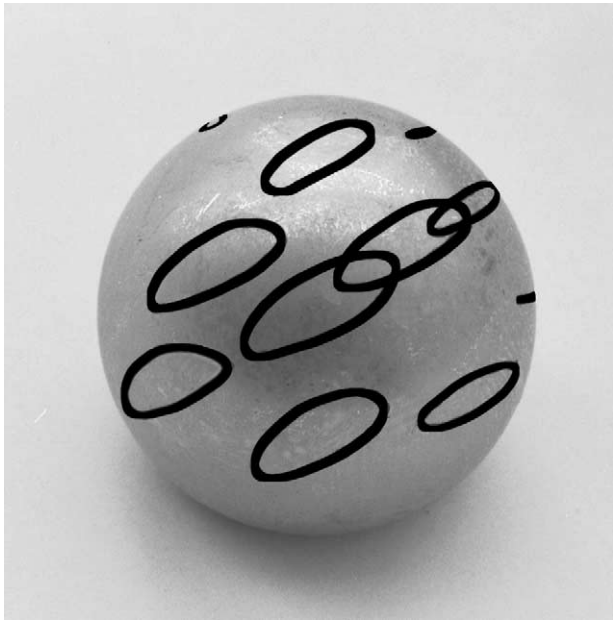

Fig. 7. Grooves engraved onto 28 mm dia. CoCr head in HUT-3 simulator. Points selected and viewing angle set as in Fig. 6(a). Grooves accentuated with ink, reflections repressed.

to that known to occur clinically (McKellop et al., 1995; Saikko et al., 2001; Wang et al., 1997). Therefore, it seems that the shapes and sizes of the slide tracks are not the only important factors. The essential point is that the direction of sliding changes continually (Fig. 11), or at least more than twice per cycle as in reciprocating motion. This is true with many different shapes: circular, elliptical, figure of eight, rectangular, etc. The fact that the BRM simulator produces realistic wear contradicts the hypothesis that the most important aspect in hip simulator design is the meticulous reproduction of motion and load waveforms of published gait studies (Viceconti et al., 1996).

At present, little is known about the effect of slide track shape on wear, apart from the basic difference between the two cases: (a) unidirectional or reciprocating motion, including also parenthesis shape, and (b) continual change of the direction of sliding, or sudden changes as in rectangular motion in the device by Bragdon et al. (1998). With protein-containing lubricant and conventional polyethylene against a polished counterface, case (a) typically yields wear factors two orders of magnitude lower than the clinical wear factors (Saikko, 1998). Case (b) meets the basic criteria, which are (I) polyethylene bearing surface becomes burnished, indicating adhesion as the principal wear mechanism, (II) wear factor is in the range $1–2 \times 10^{-6}\,mm^3/N\,m$, and (III) majority of wear particles are in the 0.1–1 μm size range (Saikko et al., 2001).

In the comparison of the wear produced by the two different hip simulators, HUT-3 and BRM (Saikko and

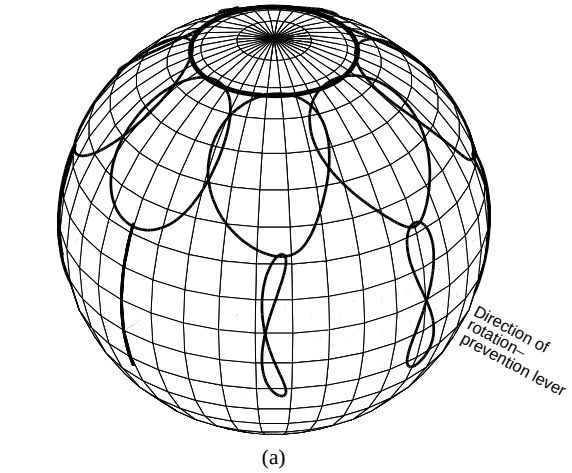

(a)

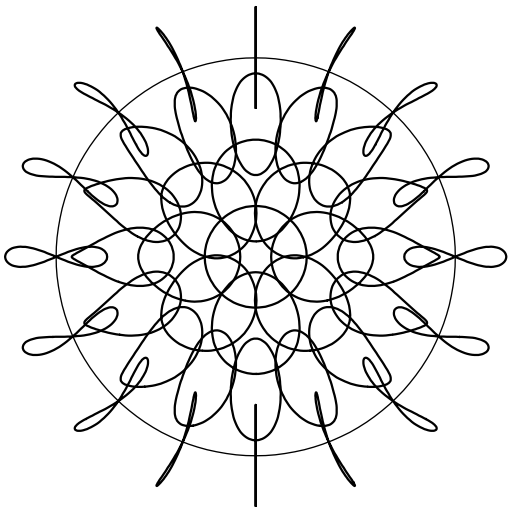

(b)

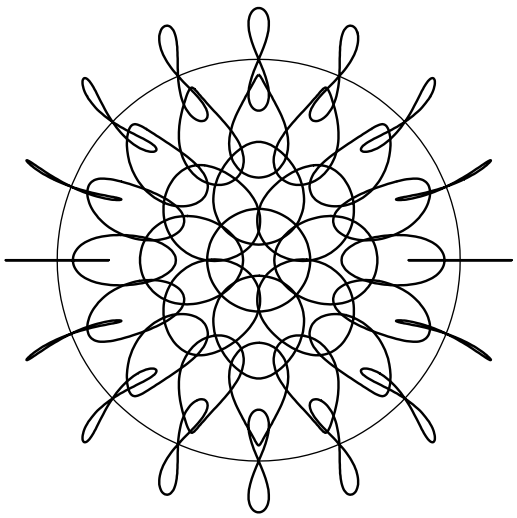

(c)

Fig. 8. Computed slide tracks of selected points for BRM simulator with zero-offset rotation-prevention lever, (a) on femoral head, and on flattened hemisphere surface of (b) femoral head and (c) acetabular cup. Flattening details as in Fig. 5.

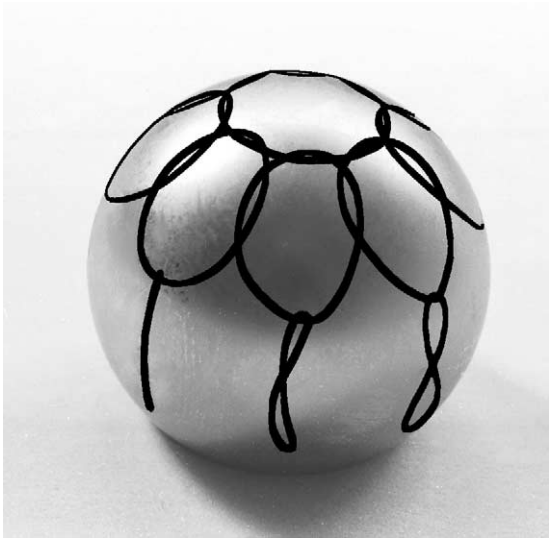

Fig. 9. Grooves engraved onto 28 mm dia. CoCr head in BRM simulator having zero-offset rotation-prevention lever. Points selected and viewing angle set as in Fig. 8 (a).

Fig. 10. Grooves engraved onto 28 mm dia. CoCr head in BRM simulator having rotation-prevention lever with 20 mm offset and rotation-prevention post with 65 mm distance from the centre of head. Engraving cup was same as in Fig. 9.

Ahlroos, 1999), it was found that using a similar load, 28 mm dia. polished CoCr head, and serum lubricant, the wear rates for conventional polyethylene cups were 11 and 22 mg/one million cycles, respectively. The fact that the wear rate produced by the BRM simulator was twice that produced by the HUT-3 simulator may be explained by the shapes of the slide tracks. In the BRM, the force track was circular (aspect ratio 1), whereas in the HUT-3, it was elliptical with an aspect ratio of 3.8. In other words, the resultant friction vector in the BRM

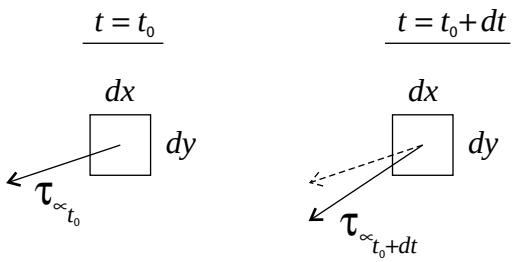

Fig. 11. Illustration of concept of constantly changing direction of sliding: infinitesimal element $dx\,dy$ of surface of acetabular cup, and change with time t of direction of frictional shear stress τ_μ which causes wear, t_0 being arbitrary moment of time during cycle. Magnitude of τ_μ may also change with time if loading is dynamic. Vector indicates instantaneous direction of tangent of slide track made on femoral head by element in question.

rotates about the load axis at nearly constant angular velocity, whereas in the HUT-3, the angular velocity of the rotation varies considerably. The elliptical shape is closer to reciprocating motion (aspect ratio ∞), which is known to result in minimal wear. Clearly, the wear decreases and finally approaches zero as the aspect ratio increases from 1 to ∞. Naturally, the contact pressure is distributed over an area of several hundred mm^2, but also the average aspect ratio of slide tracks on the load-bearing area in the BRM is smaller than that in HUT-3. Strain hardening has been proposed as an explanation for the fundamentally different wear behaviour of polyethylene in the cases of aspect ratio of 1 and ∞ (Wang et al., 1997).

The article about the computations done by the Boston group (Ramamurti et al., 1998) contains no mention of any verification. For the BRM simulator, they obtained an axisymmetric slide track pattern. Our verified results proved that the slide track pattern of the BRM simulator is not axisymmetric. For instance, the shapes of the tracks on the equator vary from figures of eight via bent figures of eight to straight lines, depending on the direction relative to the rotation-prevention lever. Between the pole and the equator, the shapes vary from egg-shaped via nonsymmetric oval to elliptic. The Boston group did not use Euler angles, but they made the rotations about fixed Cartesian coordinate axes so that the rotations were independent of each other. However, the definition of orthopaedic angles is based on Euler rotations, not on rotations about fixed coordinate axes (Andriacchi et al., 1997). Moreover, Euler rotations are well suited for the analysis of simulators, whereas a fixed Cartesian coordinate system is not, because simulators do not conform with a fixed Cartesian coordinate system.

For example, the BRM simulator with a zero-offset rotation-prevention lever is computed so that one axis, which may be called FE, is fixed, and the other axis, which may be called AA, rocks with the FE motion. Hence, the FE motion occurs about a fixed axis, and the AA motion about a sinusoidally rocking axis. Due to the peculiar mechanism of the BRM simulator, the FE and AA axes are only imaginary (not directly defined by the bearing system axes as in HUT-3 for instance), but the application of these imaginary axes makes it possible to compute the slide tracks correctly. Note that the BRM slide track pattern does not depend on whether the head moves and is located below the cup, or whether the cup moves and is located below the head. Based on the above, it is strongly recommended that in accordance with normal engineering practice, the slide track computations for simulators should be verified before publication.

Using the gait waveforms (Johnston and Smidt, 1969), the present authors computed a slide track pattern which differs from that obtained by the Boston group from exactly the same waveforms (Ramamurti et al., 1996). The difference is apparently due to the different rotation principles used, i.e., Eulerian vs. Cartesian. The present pattern is more likely to be correct because the hip simulator computations were verified, and the computation was similar in all three cases. Moreover, the present computation used 9 times more data points per cycle than that of the Boston group, resulting in a more refined visualization of the track shape.

The analysis of the uniaxial HUT-2 simulator done by the Boston group (Ramamurti et al., 1998) contains obvious errors which need to be treated. Although the analysis was actually just drawing straight lines, the length of the lines were incorrect, since the Boston group ignored the true, measured FE waveform published in the HUT-2 article (Saikko et al., 1992). Instead, they used the FE waveform by Johnston and Smidt (1969). This resulted in an underestimation of the track length by as much as 35 per cent. In addition, the track lengths using the chosen FE amplitude of 42° were miscalculated. For instance, the maximum length with 42° would be $42°/180° \times \pi \times 16\text{mm} \times 2 = 23.5\,\text{mm}$, not 21.9 mm.

The computation method developed, utilized and verified in the present study will next be applied to analyse all contemporary hip simulators. This will provide an interesting comparison, and form a sound basis for the study of the relationship between the type of multidirectional motion and the wear behaviour of prosthetic joint materials.

Acknowledgements

The study was funded by the Academy of Finland (Grant No. 43328 and Dr. Saikko's Academy Research Fellowship).

Appendix A. Computation of slide tracks

A.1. Cup track

Two coordinate systems were placed at the mutual centre of the cup and the head. The reference coordinate system XYZ was fixed relative to the cup. The axes pointed in the medial, posterior and superior directions. A moving coordinate system xyz was fixed relative to the head. The directions of the axes x, y and z with respect to the reference coordinate system were defined by the unit vectors $\mathbf{u}^1$, $\mathbf{u}^2$ and $\mathbf{u}^3$. The directions of the axes of the reference coordinate system were: $\mathbf{U}^1=[1,0,0]^T$, $\mathbf{U}^2=[0,1,0]^T$, $\mathbf{U}^3=[0,0,1]^T$. The FE, AA and IER rotations were made about the x, y and z axes according to the Euler sequence specified for the simulation. The rotation angles corresponding to the discretised FE, AA and IER waveforms were α_i, β_i, γ_i, $i=1,2,3,\ldots,N$, where N was the number of discrete points. In the present study, N was 100. A marker point P fixed to the head was repeatedly rotated from its initial position P_0 to a new position on the slide track. Each point P_i of the slide track corresponded to one set of rotation angles (α_i, β_i, γ_i). In order to avoid the accumulation of numerical errors, the points were not computed by using the previous point on the track as a starting point. For example, the rotation for the sequence FE→AA→IER was

$$\mathbf{r}_i = \mathbf{R}_{xyz}(\alpha_i, \beta_i, \gamma_i)\,\mathbf{r}_0 \tag{A.1}$$

where $\mathbf{r}_0$ was the initial position vector of the marker point, $\mathbf{r}_i$ the position vector after the rotation, and the rotation matrix $\mathbf{R}_{xyz}(\alpha, \beta, \gamma)$ was:

$$\begin{bmatrix} \cos\beta\cos\gamma & -\cos\beta\sin\gamma & \sin\beta \\ \sin\alpha\sin\beta\cos\gamma+\cos\alpha\sin\gamma & -\sin\alpha\sin\beta\sin\gamma+\cos\alpha\cos\gamma & -\sin\alpha\cos\beta \\ -\cos\alpha\sin\beta\cos\gamma+\sin\alpha\sin\gamma & \cos\alpha\sin\beta\sin\gamma+\sin\alpha\cos\gamma & \cos\alpha\cos\beta \end{bmatrix}. \tag{A.2}$$

A matrix for any sequence can be found in Craig (1989). The track was drawn by connecting all points defined by $\mathbf{r}_i$, $i=1, 2, 3, \ldots, N$. In order to check the results of the computations, an alternative method was applied for determining the slide tracks. The rotation of a point was split into three elementary rotations about the moving xyz axes. Both the position of the point and the directions of the moving axes were updated. The rotation of a point through an angle ϕ about *any* axis passing through the origin was computed as

$$\mathbf{r} = \mathbf{R}(\mathbf{u}, \phi)\,\mathbf{r}_0 \tag{A.3}$$

where the vector $\mathbf{u}=[u_x, u_y, u_z]^T$ defined the direction of the rotation axis, and the rotation matrix $\mathbf{R}(\mathbf{u}, \phi)$ was (Faux and Pratt, 1979):

$$\begin{bmatrix} u_x^2+\cos\phi(1-u_x^2) & u_xu_y(1-\cos\phi)-u_z\sin\phi & u_xu_z(1-\cos\phi)+u_y\sin\phi \\ u_yu_x(1-\cos\phi)+u_z\sin\phi & u_y^2+\cos\phi(1-u_y^2) & u_yu_z(1-\cos\phi)-u_x\sin\phi \\ u_zu_x(1-\cos\phi)-u_y\sin\phi & u_yu_z(1-\cos\phi)+u_x\sin\phi & u_z^2+\cos\phi(1-u_z^2) \end{bmatrix} \tag{A.4}$$

The alternative method was computationally less efficient, and used mainly for checking the results obtained by applying (A.1). In the vector notation used below, the superscripts correspond to the directions of the moving axes, and the subscripts denote how many times the vector has been rotated, e.g., $\mathbf{u}_0^2$ and $\mathbf{u}_1^2$ denote the initial direction, and the direction after the first rotation, of the y-axis. For example, the computations for the sequence FE→AA→IER were:

$$\mathbf{r}_{i1} = \mathbf{R}(\mathbf{u}_0^1, \alpha_i)\mathbf{r}_0, \tag{A.5}$$

$$\mathbf{u}_1^2 = \mathbf{R}(\mathbf{u}_0^1, \alpha_i)\mathbf{u}_0^2, \tag{A.6}$$

$$\mathbf{u}_1^3 = \mathbf{R}(\mathbf{u}_0^1, \alpha_i)\mathbf{u}_0^3, \tag{A.7}$$

$$\mathbf{r}_{i2} = \mathbf{R}(\mathbf{u}_1^2, \beta_i)\mathbf{r}_{i1}, \tag{A.8}$$

$$\mathbf{u}_2^3 = \mathbf{R}(\mathbf{u}_1^2, \beta_i)\mathbf{u}_1^3, \tag{A.9}$$

$$\mathbf{r}_{i3} = \mathbf{R}(\mathbf{u}_2^3, \gamma_i)\mathbf{r}_{i2}, \tag{A.10}$$

where $i=1, 2, 3, \ldots, N$, and $\mathbf{r}_0$ denoted the initial position of the marker point, and $\mathbf{r}_{i3}$ denoted the position of the marker point after the three rotations. The tracks produced by the two methods were identical.

A.2. Head track

The displacement of a marker point P, fixed to the cup, was computed from the relative orientation of the

coordinate systems XYZ and xyz, using a matrix $\mathbf{L}$ containing the direction cosines of angles between the axes:

$$\mathbf{r}_i = \mathbf{L}\mathbf{r}_0 \tag{A.11}$$

$$\mathbf{L} = \begin{bmatrix} c_{xX} & c_{xY} & c_{xZ} \\ c_{yX} & c_{yY} & c_{yZ} \\ c_{zX} & c_{zY} & c_{zZ} \end{bmatrix} \tag{A.12}$$

where, e.g., $c_{xY} = \cos(\mathbf{u}^1, \mathbf{U}^2)$ was the cosine between the axes x and Y.

For example, for the sequence FE→AA→IER, the computations were:

$$\mathbf{u}_i^1 = \mathbf{R}_{xyz}(\alpha_i, \beta_i, \gamma_i)\mathbf{u}_0^1, \tag{A.13}$$

$$\mathbf{u}_i^2 = \mathbf{R}_{xyz}(\alpha_i, \beta_i, \gamma_i)\mathbf{u}_0^2, \tag{A.14}$$

$$\mathbf{u}_i^3 = \mathbf{R}_{xyz}(\alpha_i, \beta_i, \gamma_i)\mathbf{u}_0^3. \tag{A.15}$$

Subsequently, the new position $\mathbf{r}_i$ of P was computed by applying Eq. (A.11). The process was repeated for all sets of angles (α_i, β_i, γ_i) to determine all points of the slide track. The results were checked with the alternative method, using matrix (A.4) for rotating the directions $\mathbf{u}^1$, $\mathbf{u}^2$ and $\mathbf{u}^3$. The tracks produced by the two methods were identical.

References

Andriacchi, T.P., Natarajan, R.N., Hurwitz, D.E., 1997. Musculoskeletal dynamics, locomotion, and clinical applications. In: Mow, V.C., Hayes, W.C. (Eds.), Basic Orthopaedic Biomechanics, 2nd Edition. Lippincott–Raven, Philadelphia, pp. 37–68.

Bennett, D.B., Orr, J.F., Baker, R., 2000. Movement loci of selected points on the femoral head for individual total hip arthroplasty patients using three-dimensional computer simulation. Journal of Arthroplasty 15, 909–915.

Bragdon, C.R., O'Connor, D.O., Lowenstein, J.D., Jasty, M.,Harris, W.H., 1998. Development of a new pin-on-disk testing machine for evaluating polyethylene wear. In: Proceedings of the 24th Annual Meeting of the Society for Biomaterials. San Diego, CA, USA

Craig, J.J., 1989. Introduction to Robotics: Mechanics and Control, 2nd Edition. Addison-Wesley, Reading, MA, pp. 442–443.

Dowson, D., Jobbins, B., 1988. Design and development of a versatile hip joint simulator and a preliminary assessment of wear and creep in Charnley total replacement hip joints. Engineering in Medicine 17, 111–117.

Faux, I.D., Pratt, M.J., 1979. Computational Geometry for Design and Manufacture. Ellis Horwood, Chichester, England, pp. 71–73.

Johnston, R.C., Smidt, G.L., 1969. Measurement of hip–joint motion during walking—evaluation of an electrogoniometric method. The Journal of Bone and Joint Surgery 51–A, 1083–1094.

Lewis, J.L., Lew, W.D., 1977. A note on the description of articulating joint motion. Journal of Biomechanics 10, 675–678.

McKellop, H.A., Campbell, P., Park, S.-H., Schmalzried, T.P., Grigoris, P., Amstutz, H.C., Sarmiento, A., 1995. The origin of submicron polyethylene wear debris in total hip arthroplasty. Clinical Orthopaedics and Related Research 311, 3–20.

Morrey, B.F., Chao, E.Y., 1976. Determination of three-dimensional joint motion. In: Proceedings of the 22nd Annual Meeting of the Orthopaedic Research Society. New Orleans, LA, USA.

Paul, J.P., 1976. Force actions transmitted by joints in the human body. Proceedings of the Royal Society of London B 192, 163–172.

Ramakrishnan, H.K., Kadaba, M.P., 1991. On the estimation of joint kinematics during gait. Journal of Biomechanics 24, 969–977.

Ramamurti, B.S., Bragdon, C.R., O'Connor, D.O., Lowenstein, J.D., Jasty, M., Estok, D.M., Harris, W.H., 1996. Loci of movement of selected points on the femoral head during normal gait. The Journal of Arthroplasty 11, 845–852.

Ramamurti, B.S., Estok, D.M., Jasty, M., Harris, W.H., 1998. Analysis of the kinematics of different hip simulators used to study wear of candidate materials for the articulation of total hip arthroplasties. Journal of Orthopaedic Research 16, 365–369.

Saikko, V., 1996. A three-axis hip joint simulator for wear and friction studies on total hip prostheses. Proceedings of the institution of mechanical engineers, Part H. Journal of Engineering in Medicine 210, 175–185.

Saikko, V., 1998. A multidirectional motion pin-on-disk wear test method for prosthetic joint materials. Journal of Biomedical Materials Research 41, 58–64.

Saikko, V., Ahlroos, T., 1999. Type of motion and lubricant in wear simulation of polyethylene acetabular cup. Proceedings of the institution of mechanical engineers, Part H. Journal of Engineering in Medicine 213, 301–310.

Saikko, V., Paavolainen, P., Kleimola, M., Slätis, P., 1992. A five-station hip joint simulator for wear rate studies. Proceedings of the institution of mechanical engineers, Part H. Journal of Engineering in Medicine 206, 195–200.

Saikko, V., Ahlroos, T., Calonius, O., Keränen, J., 2001. Wear simulation of total hip prostheses with polyethylene against CoCr, alumina and diamond-like carbon. Biomaterials 22, 1507–1514.

Ungethüm, M., Hildebrandt, J., Jäger, M., Moslé, H.G., 1973. Ein neuer Simulator zur Testung von Totalendoprothesen für das Hüftgelenk. Archiv für orthopädische und Unfall-Chirurgie 77, 304–314.

Viceconti, M., Cavallotti, G., Andrisano, A.O., Toni, A., 1996. Discussion on the design of a hip joint simulator. Medical Engineering and Physics 18, 234–240.

Wang, A., Sun, D.C., Yau, S.S., Edwards, B., Sokol, M., Essner, A., Polineni, V.K., Stark, C., Dumbleton, J.H., 1997. Orientation softening in the deformation and wear of ultra-high molecular weight polyethylene. Wear 203–204, 230–241.